Picosecond linear vibrational spectroscopy of CO adsorbed on Cu(111) by phase-sensitive polarization modulation

A. G. Yodh* and H. W. K. Tom
AT&T Bell Laboratories, Holmdel, New Jersey 07733
(Received 20 December 1991)

We have measured the linear absorption at 2074 cm^{-1} of CO adsorbed on Cu(111) with a laser-based picosecond infrared (ir) source operating at 76 MHz. In order to overcome relatively large source fluctuations that hinder this and similar ir experiments, we have developed a polarization-modulation technique that enables us to measure $\sim 1\%$ changes in reflection with a signal-to-noise ratio of 10 in approximately 1 min. The measurements are described, and a full theory for these experiments is presented.

Vibrational spectroscopy of simple molecular adsorbates on clean metal surfaces is important for a variety of fundamental and technological reasons. Fourier-transform infrared methods[1] have played a major role in many investigations, and more recently time-resolved infrared (ir) experiments on the picosecond time scale[2–4] have provided additional information on energy flow and dephasing phenomena in these two-dimensional systems. Linear reflection spectroscopy is probably the simplest of all vibrational probes. Unfortunately, the small absorptions of monolayer systems coupled with the relatively noisy laser-based infrared sources[5–13] make simple linear measurements in the short-time regime difficult to perform.

We have measured the linear absorption of the atop resonance at 2074 cm^{-1} of CO adsorbed to Cu(111) with a laser-based picosecond ir source operating at 76 MHz.[14] A polarization-modulation scheme was developed to carry out these experiments. The scheme enabled us to measure $\sim 1\%$ changes in reflection with a signal-to-noise ratio of ~ 10 in one minute. The method can be used on slow time scales to provide information about surface chemical reactions and kinetic phenomena, and it can be integrated into more complex short pulse pump-probe ir schemes to provide quick measurements of adsorbate coverage.

Our method is ellipsometric in character.[15] Infrared ellipsometry was extensively developed in the mid 1970s,[15–18] and has been used to provide information on surface phenomena with considerable success.[19] The probe discussed here differs from other infrared ellipsometric probes[15–18,20] in several ways. (1) The apparatus is designed for use with laser-based ir sources rather than lamps. The laser-based sources are essential for time-resolved work, but are much nosier than lamps. Detector noise is not a significant problem in laser experiments since the ir sources are very bright. On the other hand, the laser experiments are prone to a substantial number of new systematics that can degrade the experimental signal-to-noise ratio. Our detection scheme deals with these problems directly. (2) The setup employs a different polarization configuration (a fixed input polarizer and a rotating output polarizer), and offers direct access to the sample absorption with a single lock-in amplifier. Since the scheme does not directly measure absorption amplitudes, isotropic absorbers in the beam path do not affect the measurement. (3) The apparatus does not require background subtraction or digital filtering and averaging techniques. Presently we will describe the measurement, analyze the information contained in these signals, and present our experimental results.

THEORY

A schematic of the experimental setup is shown in Fig. 1. An infrared light beam is polarized (with approximately equal amounts of *s*- and *p*-polarization components), and then directed onto a metal substrate containing chemisorbed CO. A portion of the light is specularly reflected from the metal surface, passed through a rotating polarizer, and then focused onto a square-law detector. The detected light intensity varies sinusoidally in time. We measure the phase shift of this sinusoid as a function of ir frequency. When the ir beam is resonant with the CO stretch mode frequency, the molecules absorb energy from the beam. In practice, CO only absorbs energy from the *p*-polarized component of the incident beam. Thus, when the ir beam is on resonance, the reflected polarization is rotated with respect to the input beam polarization, causing a shift in the intensity null of

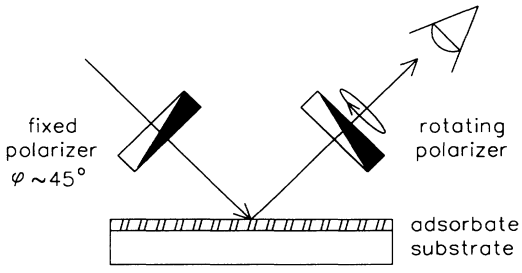

FIG. 1. Schematic of the polarization-modulation experiment. A tunable ir beam is polarized and directed onto a sample consisting of an adsorbate and a substrate. The input beam is polarized with approximately equal amounts of *s*- and *p*-polarized components. The specularly reflected output beam is directed through a rotating polarizer, and then detected.

the detected light. The measured phase shift is independent of temporal laser fluctuations, and frequency-dependent variations of the source and detector efficiency. With this overview in mind, we shall calculate the phase shift starting from elementary considerations.

We model our sample as three adjoined linear media. Medium one is the vacuum, medium two is the metal, and medium three is the monolayer of CO molecules adsorbed to the metal surface. The monolayer perturbs the optical properties of the system, but we assume throughout this discussion that this perturbation is very weak. The three media are characterized by frequency-dependent dielectric constants ϵ_1, ϵ_2, and ϵ_3, respectively. An incident electric field, $\mathbf{E}_i$, impinges from vacuum onto the metal surface. The incident electric field is passed through a polarizer, and has both *s*- and *p*-polarization components. Just before it reaches the metal surface, $\mathbf{E}_i$ can be written in the form

$$\mathbf{E}_i = E_0(\cos\phi \mathbf{e}_p + \sin\phi \mathbf{e}_s)\exp\{i\mathbf{k}_1\cdot\mathbf{r} - i\omega' t\} , \tag{1}$$

where E_0 is the incident field amplitude, ϕ is an angle determined by the input polarizer that will be optimized later, $\mathbf{e}_s$ ($\mathbf{e}_p$) is a unit vector along the *s*- (*p*-) polarization direction, ω' is the carrier frequency of the wave, and $\mathbf{k}_1$ is the incident wave vector. In general, we have $|\mathbf{k}_i| = k_i = (\omega'/c)\sqrt{\epsilon_i}$, and we choose our coordinate system so that the xz plane is the plane of incidence. The z axis is normal to the surface, and its positive direction is taken to point into the surface.

The electric field *in* the monolayer is determined using the Fresnel reflection amplitudes for the vacuum-metal interface. If we ignore interactions between the adsorbate layer and the metal, then we can approximate this field by the sum of the incident and reflected fields just above the metal surface. The components of the electric field in the adsorbate layer are thus

$$E_x = E_0\cos\phi(r_p - 1)(k_{1z}/k_1) , \tag{2a}$$

$$E_y = E_0\sin\phi(r_s + 1) , \tag{2b}$$

$$E_z = E_0\cos\phi(r_p + 1)(k_{1x}/k_1) , \tag{2c}$$

where r_p (r_s) is the *p*-polarized (*s*-polarized) complex reflection amplitude, and k_{ix}, k_{iy}, k_{iz} represent the components of $\mathbf{k}_i$ along the x,y,z axes, respectively. The Fresnel reflection amplitudes are

$$r_p = (\epsilon_2 k_{1z} - \epsilon_1 k_{2z})/(\epsilon_2 k_{1z} + \epsilon_1 k_{2z}) , \tag{3a}$$

$$r_s = (k_{1z} - k_{2z})/(k_{1z} + k_{2z}) . \tag{3b}$$

The polarization $\mathbf{P}$ produced in the adsorbate monolayer depends linearly on the field given in Eq. (2), i.e., $\mathbf{P} = \chi\mathbf{E}$. χ is the linear susceptibility of the monolayer. If the molecules in the adsorbate layer do not interact, then $\chi = N\alpha$, where N is the number of molecules per unit area, and α is the molecular polarizability of the individual molecules. We assume the molecules *do* interact and continue to use the more general layer susceptibility χ. In many problems of practical interest, the adsorbates will have azimuthal symmetry with respect to the surface normal so that $\chi_{xx} = \chi_{yy} = \chi_\parallel$, $\chi_{zz} = \chi_\perp$, and $\chi_{ij} = \chi_{ij}\delta_{ij}$. Under these circumstances the components of the monolayer polarization are

$$P_x = \chi_\parallel E_0\cos\phi(r_p - 1)(k_{1z}/k_1) , \tag{4a}$$

$$P_y = \chi_\parallel E_0\sin\phi(r_s + 1) , \tag{4b}$$

$$P_z = \chi_\perp E_0\cos\phi(r_p + 1)(k_{1x}/k_1) . \tag{4c}$$

The total reflected field arises as a result of two contributions. One contribution is from the metal, and is determined by the Fresnel amplitudes r_p and r_s. The other contribution is from the monolayer. We model the monolayer as a sheet of polarization with components P_x, P_y, P_z. The electric field radiated by such a polarized sheet is found by solving Maxwell's equations.[21,22] The resulting *p*-polarized ($E_{p,a}$) and *s*-polarized ($E_{s,a}$) far-field electric-field components of the *adsorbate* response are

$$E_{p,a} = [i4\pi k_1/(\epsilon_2 k_{1z} + \epsilon_1 k_{2z})][k_{2z}P_x + (\epsilon_2/\epsilon_3)k_{1x}P_z] , \tag{5a}$$

$$E_{s,a} = [i4\pi k_1/(k_{1z} + k_{2z})][(k_1/\epsilon_1)P_y] . \tag{5b}$$

For the present problem we have $\epsilon_1 = 1$, and we take $\epsilon_3 = \epsilon_1$ [this choice of ϵ_3 always implicitly modifies $\chi_\perp$, e.g., by a factor of $(1/\epsilon_3)^2$ for $\chi_\perp$]. The corresponding *adsorbate* reflection amplitudes $r_{p,a}$ and $r_{s,a}$ are computed by dividing $E_{p,a}$ and $E_{s,a}$ by the *p* and *s* components of $\mathbf{E}_i$.

Using Eqs. (4) and (5), we can determine the *total* *p*- and *s*-polarized reflected field amplitudes $r_{p,\mathrm{tot}}$ and $r_{s,\mathrm{tot}}$. The *p*-polarized (*s*-polarized) total amplitude is the sum of r_p and $r_{p,a}$ (r_s and $r_{s,a}$). After some algebra we find

$$r_{s,\mathrm{tot}} = r_s\{1 + [i8\pi k_{1z}/(\epsilon_1 - \epsilon_2)]\chi_\parallel\} , \tag{6a}$$

$$r_{p,\mathrm{tot}} = r_p(1 + \{i8\pi k_{1z}/[(\epsilon_2 k_{1z})^2 - (\epsilon_1 k_{2z})^2]\} \times(\epsilon_2^2 k_{1x}^2\chi_\perp - \epsilon_1 k_{2z}^2\chi_\parallel)) . \tag{6b}$$

Equation (6) is a general result for reflection from a metal with an azimuthally symmetric adsorbate layer. We will now specialize to the case of CO adsorbed on Cu(111). A more general set of results is given in the Appendix. CO is known to adsorb perpendicular to the metal surface with the C down. Thus, the CO stretch vibration has its dipole moment perpendicular to the surface, $\chi_\parallel = 0$, and only $r_{p,\mathrm{tot}}$ is modified as a result of the adsorbate layer:

$$r_{p,\mathrm{tot}} = r_p(1 + iG\chi_\perp) , \tag{7a}$$

$$r_{s,\mathrm{tot}} = r_s , \tag{7b}$$

and

$$G = 8\pi k_{1z}k_{1x}^2/[k_{1z}^2 - (\epsilon_1/\epsilon_2)^2 k_{2z}^2] . \tag{7c}$$

The function G has been derived by several authors.[23–25,1] It depends on angle of incidence, and usually has a maximum for angles greater than 80°. For metals irradiated in the ir, G is predominantly real. However at very high incidence angles (e.g., 89°), G often acquires a small phase shift of $\sim 10°$. The magnitude of this phase

shift will vary from metal to metal and will become larger as the probe wavelength shifts to the blue.

In standard ir reflectance measurements, one measures the differential reflectivity,

$$\Delta R/R = |(r_{p,\mathrm{tot}})^2 - r_p^2|/r_p^2 , \tag{8}$$

due to the adsorbate layer. If G is real and $\chi_\perp$ is small, then $\Delta R/R = -2G\,\mathrm{Im}\{\chi_\perp\}$, and one obtains information on the absorption of the adsorbate layer. Clearly one would like to choose an incidence angle that maximizes G. The variation of G as a function of incidence angle for Pt at photon energies of 0.25 eV is given in Ref. 25. For Pt at this energy, $\epsilon = -300 + i190$, and G has a sharp maximum at approximately 85°. The more general case of complex G is not usually considered. It is not widely recognized, for example, that the measured line shapes will have asymmetries due to a mixture of adsorbate absorption and dispersion that arise when G is complex. This scenario can arise at *high incidence angles,* and perhaps more importantly, it can arise in *pump-probe experiments* if the pump pulse modifies the substrate dielectric constant.

In our polarization modulation experiments, we operate at lower incidence angles ($< 80°$), where G is fairly large and real. The light reflected from the sample surface is passed through a polarizer that rotates with angular frequency ω, and is then detected. The pass axis of the polarizer, $\mathbf{e}_{\mathrm{pass}}$, changes in time and is given by

$$\mathbf{e}_{\mathrm{pass}} = \cos(\omega t)\mathbf{e}_p + \sin(\omega t)\mathbf{e}_s . \tag{9}$$

The reflected field amplitude is

$$\mathbf{E}_{\mathrm{ref}} = E_0(r_{p,\mathrm{tot}}\cos\phi\mathbf{e}_p + r_{s,\mathrm{tot}}\sin\phi\mathbf{e}_s) , \tag{10}$$

and the normalized intensity I_T/I_o transmitted through the output polarizer is

$$I_T/I_o = |\mathbf{E}_{\mathrm{ref}}\cdot\mathbf{e}_{\mathrm{pass}}|^2/|E_0|^2$$

$$= |r_{p,\mathrm{tot}}\cos\phi\cos(\omega t) + r_{s,\mathrm{tot}}\sin\phi\sin(\omega t)|^2 . \tag{11}$$

We can write I_T/I_o in the form

$$I_T/I_o = A + B\sin(2\omega t + \Psi) , \tag{12}$$

where A, B, and Ψ depend on the specific conditions one is considering. For example, evaluation of Eq. (11) for the *bare metal* with the polarizers set so that $r_p^2\cos^2\phi = r_s^2\sin^2\phi$ gives

$$A = r_p^2\cos^2\phi , \tag{13a}$$

$$B = \tfrac{1}{2}\sin(2\phi)\mathrm{Re}(r_p^* r_s) = A , \tag{13b}$$

and

$$\Psi = 0 . \tag{13c}$$

When we add adsorbates to the metal surface, then r_p changes to $r_{p,\mathrm{tot}} = r_p\{1 + iG\chi_\perp\}$, and (again with polarizers set so that $r_p^2\cos^2\phi = r_s^2\sin^2\phi$) we find that

$$A = \tfrac{1}{2}(|r_p|^2|1 + iG\chi_\perp|^2\cos^2\phi + |r_s|^2\sin^2\phi) , \tag{14a}$$

$$\tan\Psi = \frac{|r_p|^2|1 + iG\chi_\perp|^2\cos^2\phi + |r_s|^2\sin^2\phi}{\sin(2\phi)\,\mathrm{Re}[r_p r_s^*(1 + iG\chi_\perp)]} , \tag{14b}$$

$$B = \tfrac{1}{2}\sin(2\phi)\mathrm{Re}[r_p r_s^*(1 + iG\chi_\perp)](1 + \tan\Psi)^{1/2} . \tag{14c}$$

Equations (14) are algebraically complex, but they simplify dramatically in practice. If $|G\chi_\perp| \ll 1$, and r_p/r_s is real, then the phase shift Ψ is

$$\Psi = -2\,\mathrm{Im}\{G\chi_\perp\} . \tag{15}$$

When G is real, this reduces to the oft-quoted result for a typical differential reflectivity measurement.[1,25] The amplitudes A and B simplify also, but the utility of our method arises because it is very easy to measure the phase shift.

Figure 2 shows schematically the transmitted intensity as a function of time. With no adsorbate absorption (i.e., ir off resonance) the signal will oscillate sinusoidally in time (solid line in Fig. 2). When the ir beam is tuned to the adsorbate resonance, we observe a number of small changes (dashed line in Fig. 2). Most importantly, we see that the *phase* of the sinusoidal oscillation shifts by an amount given in Eq. (15). That is, the position of the minima of the sinusoid shifts in time. Second, we notice that both the dc and ac *amplitudes* change. These changes depend on the absorptive *and* dispersive part of the adsorbate response, so that in principle we can derive both the absorptive and dispersive parts of the adsorbate susceptibility with our technique.

The voltage produced by the ir detector has a dc component, as well as an in-phase and in-quadrature ac component oscillating at 2ω. Using commercially available vector lock-in amplifiers, it is possible to take a reference signal oscillating at 2ω, and simultaneously measure the in-phase and in-quadrature components of the ac ir signal. Although the dc component of our transmitted intensity is lost, one can determine the phase shift Ψ direct-

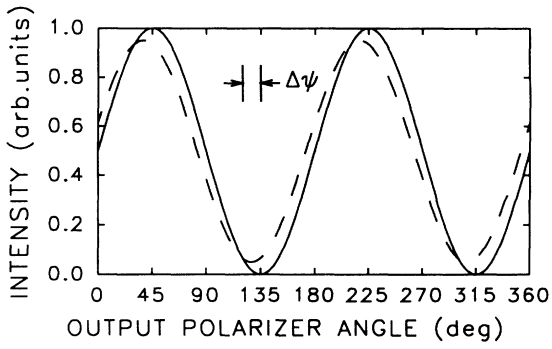

FIG. 2. Schematic variation of ir intensity as measured by the detector after the rotating polarizer. The solid line represents the measured signal intensity when the ir beam is not on resonance. The dashed line represents the measured signal intensity when the ir beam resonantly excites the adsorbate and is partially absorbed. In this case, we see that the reflected amplitude decreases, and that the phase of the oscillation shifts. In our experiment, we detect this phase shift as a function of ir frequency.

ly from this information. Because the phase shift involves a ratio of the two signal components it is independent of the input field strength. All source fluctuations arise with equal magnitude in both quadratures, and are normalized without a second detector. This includes temporal intensity fluctuations and frequency-dependent systematic effects associated with the source and detection system. This latter feature is especially important for laser-based ir sources, because the noise in any measurement of Ψ is only limited by the source amplitude noise at 2ω, within a bandwidth set by the lock-in averaging time.

EXPERIMENT

A schematic of the experimental apparatus is shown in Fig. 3. The experiment has three distinct components: (1) ir generation, (2) sample in ultrahigh vacuum, and (3) ir detection. We discuss each component separately, and then describe the systematic problems (along with our solutions) that arise when we combine parts.

The ir generation scheme we have used has been previously described.[14] The apparatus produces tunable infrared pulses from 3.4 to 7.0 μm by difference frequency mixing in $AgGaS_2$. The last step of this process is shown in Fig. 3. The pulses are ~ 2.2 psec in duration, have a frequency bandwidth of ~ 6.6 cm^{-1}, and are produced at a 76-MHz repetition rate. Approximately 5 μW of ir average power is incident on the Cu sample.

Unfortunately in our scheme, as well as in almost any method that employs nonlinear optics to generate ir, the temporal intensity fluctuations are not small. For example, we produce the ir by mixing picosecond pulses from a synchronously pumped dye laser with optical fiber-compressed pulses at 1.06 μm, derived from a mode-locked Nd-yttrium-aluminum-garnet (YAG) laser. Typical YAG laser intensity fluctuations of only 2% result in $>10\%$ variations in the ir. As an example, our ir fluctuations at 100 Hz were still $\sim 10\%$ with one-second averaging time constants. These short-term fluctuations can be reduced by longer averaging time constants, provided that there are no serious long-term drifts. A more insidious set of problems are the variation in power, mode quality, and beam pointing that arise as one spectrally tunes the ir source. We will return to these problems after describing the vacuum and detection systems.

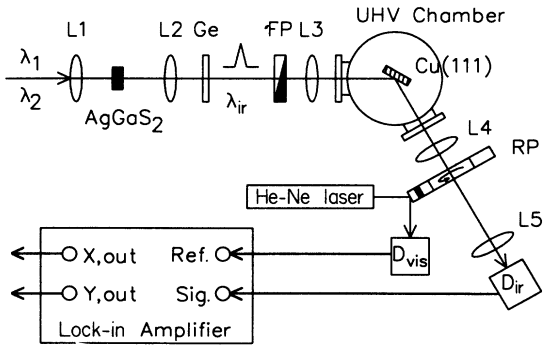

FIG. 3. Detailed schematic of experimental setup. Two near-ir pulses with wavelengths λ_1 and λ_2 are downconverted in $AgGaS_2$ to produce picosecond pulses with wavelength λ_{ir}. A germanium plate (Ge) separates the ir from the source pulses. The ir beam is polarized, directed onto a Cu(111) crystal residing in the UHV chamber, and then collected through the rotating output polarizer. Light from a He-Ne laser is used to provide a reference for lock-in detection of the reflected ir. The phase shift of the reflected ir is computed from the in-phase (X) and in-quadrature (Y) outputs of the lock-in amplifier. $L1$–$L5$, lenses; FP, fixed ir polarizer; RP, rotating ir polarizer; D_{ir}, $Hg_{1-x}Cd_xTe$ ir detector; D_{vis}, photodiode to detect visible beam.

Our sample consists of approximately $\frac{1}{3}$ monolayer of CO adsorbed on the atop sites of Cu(111) in ultrahigh vacuum ($\sim 1\times 10^{-10}$ Torr) at 110 K. The vacuum chamber was equipped with standard surface instrumentation so that we were able to perform Auger electron spectroscopy, low-energy electron diffraction (LEED), as well as clean the Cu by sputtering and annealing. The Cu(111) sample was initially prepared by alternate Ar^+ ion sputtering at 400 eV, and thermal annealing at 350 °C, for 15 min, until LEED measurements exhibited a sharp 1×1 pattern, and the Auger spectra showed less than 0.5% P, B, and S. At these levels, C and O were undetectable. The CO layer was prepared by dosing 6 L of CO onto the clean Cu surface at 90 K, and then allowing the surface temperature to rise to 110 K. This annealing process produced sharp $(\sqrt{3}\times\sqrt{3})R30°$ LEED patterns corresponding to $\frac{1}{3}$ monolayer occupying atop sites.[26,27]

The chamber was equipped with CaF_2 windows to transmit the ir beams with minimal loss and depolarization. The substrate was oriented to provide an angle of incidence of 71°, and the ir spot size on the sample was 0.5 mm. The polarizers (both fixed input and rotating output) were located outside the chamber, and provided an extinction ratio of $\sim 1/200$ consistent with the expected performance of wire grid polarizers. Depolarization by the windows, and other optical components, were observed to be $<1\%$. Depolarization due to the clean sample was calculated to be far less than 1%.

As noted earlier, the input polarization was set at an angle of $\sim 45°$ with respect to the plane of incidence, and the reflected output was passed through a rotating polarizer. A belt-driven motor assembly was used to force the polarizer to rotate at a rate of 200 revolutions per second. The transmitted light was then detected with a commercial liquid-nitrogen-cooled $Hg_{1-x}Cd_xTe$ detector-amplifier system. The detected output was fed into a two-phase lock-in amplifier. The lock-in reference signal was derived from a He-Ne laser beam that reflected off a marked position on the rotating polarizer mount. In this way, any mechanical slippage of the polarizer was experienced simultaneously by the reference and the ir beam. The He-Ne signal was detected with a photodiode and its ac intensity variation was used to produce the lock-in reference.

As described above [see Eq. (15)] the phase shift of the signal intensity oscillating at 2ω was then measured as a function of ir frequency between 2024 and 2104 cm^{-1}. The CO resonance feature is shown in Fig. 4(a). The en-

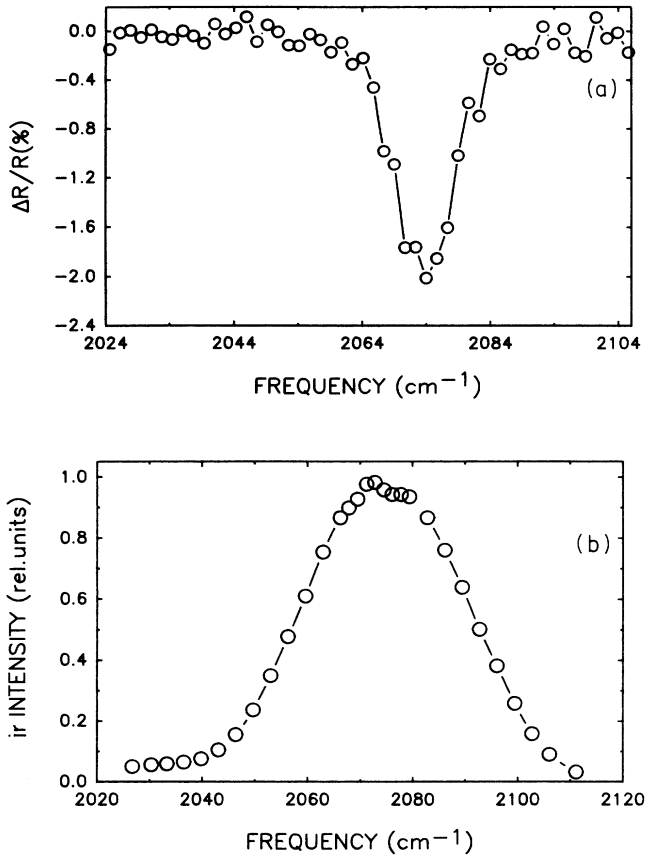

FIG. 4. (a) Differential reflectance as a result of CO absorption as a function of ir frequency. (b) Variation of the incident ir intensity as a function of ir frequency over the same frequency range.

tire spectrum was taken in one minute (1.5 sec per frequency point). It corresponds to a differential p-polarized reflectivity ($\Delta R/R$) of $\sim 2\%$ at peak. The noise level is $\sim 2\times 10^{-3}$, and is limited by the laser noise at 2ω. The observation of the atop CO resonance at 2074 cm^{-1}, and the absence of detectable bridge-bonded CO at 1830 cm^{-1}, were consistent with Ref. 26. The resonance bandwidth is 11.3 cm^{-1}. Since the bandwidth [full width at half maximum (FWHM)] of our ir source was 6.6 cm^{-1}, we deduce that the CO resonance has a natural linewidth of 9.2 cm^{-1}. This prediction is consistent with the literature values[26,27] at these temperatures and coverages. In order to improve the frequency resolution of our measurements, we can simply use ir pulses with longer temporal durations.

The apparatus described works very well, particularly at fixed ir frequency. If one wants to measure a line shape, however, a variety of systematic effects can degrade the measurement. Wavelength-dependent changes in transmission through the optics and vacuum system are not important, since our resonances are quite sharp. Similarly, wavelength-dependent changes in overall detector efficiency are not very severe when only a single $Hg_{1-x}Cd_xTe$ detector is involved.

On the other hand, ir beam movement on the substrate surface causes signal fluctuation, since the reflection amplitudes, and G, depend strongly on incidence angle. We minimize this systematic by scanning the ir frequency at a *fixed* angle of the nonlinear crystal. Under these circumstances, the ir intensity was observed to vary by a factor of ~ 10 over a 90-cm^{-1} interval [see Fig. 4(b)]. While the amplitude change by itself was normalized by the phase measurements, other systematics caused by beam pointing produced errors. These variations arise because, at fixed crystal angle, both the optimum $AgGaS_2$ phase matching condition and the transverse beam profile depend on ir frequency.[28] Ultimately, these variations brought about transmission changes through the wire grid polarizers, and modified detection efficiencies when different portions of the $Hg_{1-x}Cd_xTe$ detector surface were illuminated.

We reduced these effects by directly imaging the interaction spot in the $AgGaS_2$ crystal onto the polarizers, sample, and detector. The effects of small variations in transverse mode quality and propagation direction were thus minimized, because (to first order) the ir beam passes through the same position on all critical devices in the system. The only other beam pointing instability arose as a result of sample rotation. This problem was minimized by allowing the entire sample manipulator assembly to come into thermal equilibrium before starting the measurements. Thus, in Fig. 4(a), we observe a clean CO resonance over a flat base line. We found that if we did not image the interaction spot, and we did not wait for the sample manipulator to achieve thermal equilibrium, then the base line might change by as much as 20% over the same range.

In conclusion, we have discussed and demonstrated a phase-sensitive polarization-modulation scheme that enables us to measure the linear absorption properties of adsorbates on metal surfaces with high sensitivity. A more conventional reflectivity measurement [see Eq. (8)] without background subtraction, but with the same laser fluctuations, would require $\sim 10^6$ sec to achieve the same signal-to-noise ratio. The method can be used as part of more complex picosecond and subpicosecond, high-repetition-rate, pump-probe schemes to provide quick and accurate measurements of sample properties such as coverage. Perhaps more importantly, the method can be used on slow time scales to provide information about surface chemical reactions, surface diffusion, and other kinetic phenomena. For example, time-resolved Fourier transform infrared (FTIR) (Ref. 29) has provided information about CO migration from terraces to steps. The resolution of these experiments is ~ 1 msec. Similar information can be obtained from fast *single-frequency* ir scans using the apparatus we have described, but with slightly faster (~ 10 times) modulation frequencies. With commercial motors and gearing, an increase in modulation frequency by at least a factor of 20 should be possible.

ACKNOWLEDGMENTS

We are pleased to acknowledge the technical assistance provided by G. D. Aumiller in many aspects of this work.

A.G.Y. gratefully acknowledges partial support from the NSF through the PYI program No. DMR-9058498.

APPENDIX: RESULTS FOR ADSORBATE LAYERS WITH FULL AZIMUTHAL SYMMETRY

In this appendix, we calculate the normalized output intensity for the case of adsorbates with full azimuthal symmetry (e.g., $\chi_\parallel$ is not zero). Our starting point for the calculation is Eq. (6) of the main text. Equation (6) provides the full expressions for the total p- and s-polarized reflected field amplitudes,

$$r_{s,\mathrm{tot}}=r_s\{1+[i8\pi k_{1z}/(\epsilon_1-\epsilon_2)]\chi_\parallel\}\ , \tag{6a}$$

$$r_{p,\mathrm{tot}}=r_p(1+\{i8\pi k_{1z}/[(\epsilon_2 k_{1z})^2-(\epsilon_1 k_{2z})^2]\}\times(\epsilon_2^2 k_{1x}^2\chi_\perp-\epsilon_1 k_{2z}^2\chi_\parallel))\ . \tag{6b}$$

We first rewrite Eq. (6) in terms of a new set of G factors,

$$r_{s,\mathrm{tot}}=r_s\{1+iG_s\chi_\parallel\}\ , \tag{A1a}$$

$$r_{p,\mathrm{tot}}=r_p\{1+iG_\perp\chi_\perp+iG_\parallel\chi_\parallel\}\ , \tag{A1b}$$

where

$$G_s=8\pi k_{1z}/(\epsilon_1-\epsilon_2)\ , \tag{A2a}$$

$$G_\perp=8\pi k_{1z}k_{1x}^2/[(k_{1z})^2-(\epsilon_1/\epsilon_2)^2k_{2z}^2]\ , \tag{A2b}$$

$$G_\parallel=-8\pi\epsilon_1 k_{2z}^2k_{1z}/[(k_{1z})^2-(\epsilon_1/\epsilon_2)^2k_{2z}^2]\ . \tag{A2c}$$

The next part of the calculation is the same as in the main text. We determine the normalized transmitted intensity through the rotating polarizer, and find that

$$I_T/I_o=A+B\sin(2\omega t+\Psi)\ , \tag{A3a}$$

where

$$A=\tfrac{1}{2}(|r_p|^2|1+iG_\parallel\chi_\parallel+iG_\perp\chi_\perp|^2\cos^2\phi+|r_s|^2|1+iG_s\chi_\parallel|^2\sin^2\phi)\ , \tag{A3b}$$

$$\tan\Psi=\frac{|r_p|^2|1+iG_\perp\chi_\perp+iG_\parallel\chi_\parallel|^2\cos^2\phi+|r_s|^2|1+iG_s\chi_\parallel|^2\sin^2\phi}{\sin(2\phi)\mathrm{Re}[r_pr_s^*(1+iG_\perp\chi_\perp+iG_\parallel\chi_\parallel-iG_s^*\chi_\parallel^*+G_\parallel G_s^*\chi_\parallel\chi_\parallel^*+G_\perp G_s^*\chi_\perp\chi_\parallel^*)]}\ , \tag{A3c}$$

$$B=\tfrac{1}{2}\sin(2\phi)\mathrm{Re}[r_pr_s^*(1+iG_\perp\chi_\perp+iG_\parallel\chi_\parallel-iG_s^*\chi_\parallel^*+G_\parallel G_s^*\chi_\parallel\chi_\parallel^*+G_\perp G_s^*\chi_\perp\chi_\parallel^*)](1+\tan\Psi)^{1/2}\ . \tag{A3d}$$

This result can be further simplified when the $|G\chi|\ll 1$, r_p/r_s is real, and we choose ϕ so that $r_p^2\cos^2\phi=r_s^2\sin^2\phi$. In this case our phase shift will give information on the parallel and perpendicular parts of the adsorbate susceptibility.

*Present address: Department of Physics, University of Pennsylvania, Philadelphia, PA 19104.

[1]For a general reference on surface infrared spectroscopy, see Y. J. Chabal, Surf. Sci. Rep. **8**, 211 (1988).

[2]See, for example, D. A. King, N. V. Richardson, and S. Holloway, *Vibrations at Surfaces, 1985* (Elsevier, Amsterdam, 1986).

[3]J. D. Beckerle, M. P. Casassa, R. R. Cavanaugh, E. J. Heilwiel, and J. C. Stephenson, Phys. Rev. Lett. **64**, 2090 (1990).

[4]A. L. Harris, L. Rothberg, L. H. Dubois, N. J. Levinos, and L. Dhar, Phys. Rev. Lett. **64**, 2086 (1990); P. Guyot Sionnest, P. Dumas, Y. J. Chabal, and G. S. Higashi, *ibid.* **64**, 2156 (1990).

[5]T. Elsaesser, H. Lobentanzer, and A. Seilmeier, Opt. Commun. **52**, 355 (1985); A. Seilmeier, K. Spanner, A. Laubereau, and W. Kaiser, *ibid.* **24**, 237 (1978); T. Elsaesser, A. Seilmeier, W. Kaiser, P. Koidl, and G. Brandt, Appl. Phys. Lett. **44**, 383 (1984).

[6]T. M. Jedju and L. J. Rothberg, Appl. Opt. **26**, 2877 (1987).

[7]D. S. Moore and S. C. Schmidt, Opt. Lett. **12**, 480 (1987).

[8]J. H. Glownia, J. Misewich, and P. P. Sorokin, Opt. Lett. **12**, 19 (1987).

[9]M. Berg, A. L. Harris, J. K. Brown, and C. B. Harris, Opt. Lett. **9**, 50 (1984).

[10]J. N. Moore, P. A. Hansen, and R. M. Hochstrasser, Chem. Phys. Lett. **138**, 110 (1987); P. A. Hansen, J. N. Moore, and R. M. Hochstrasser, Chem. Phys. **131**, 49 (1989); P. Anfinrud, C. Han, P. A. Hansen, J. N. Moore, and R. M. Hochstrasser, in *Ultrafast Phenomena VI,* edited by T. Yajima, K. Yoshihara, C. B. Harris, and S. Shionoya (Springer-Verlag, Berlin, 1988), p. 442.

[11]P. C. Becker, D. Gershoni, and A. Prosser, in *Ultrafast Phenomena VII,* edited by C. B. Harris, E. Ippen, G. Mourou, and A. Zewail (Springer-Verlag, Berlin, 1990), p. 81; T. Elsaesser and M. C. Nuss, *ibid.*, p. 85.

[12]I. S. Ruddock, R. Illingworth, and L. Reekie, Opt. Quantum Electron. (U.K.) **16**, 87 (1984).

[13]H. Vanherzeele, Appl. Opt. **29**, 2246 (1990).

[14]A. G. Yodh, H. W. K. Tom, G. D. Aumiller, and R. S. Miranda, J. Opt. Soc. Am. B **8**, 1663 (1991).

[15]See, for example, D. E. Aspnes, J. Opt. Soc. Am. **64**, 812 (1974); **64**, 639 (1974); D. E. Aspnes and A. A. Studna, Appl. Opt. **14**, 220 (1975), and references therein.

[16]M. J. Dignam, B. Rao, and R. W. Stobie, Surf. Sci. **46**, 308 (1974).

[17]P. Hoffman, R. Unwin, W. Wyrobisch, and A. M. Bradshaw, Surf. Sci. **72**, 513 (1977).

[18]W. Golden, D. S. Dunn, and J. Overend, J. Phys. Chem. **82**, 843 (1978).

[19]See, for example, J. D. Fedyk, P. Mahaffy, and M. J. Dignam, Surf. Sci. **89**, 404 (1979).

[20]D. S. Bethune, M. D. Williams, and L. C. Luntz, J. Chem. Phys. **88**, 3322 (1988).

[21]N. Bloembergen and P. S. Pershan, Phys. Rev. **128**, 606 (1962).

[22]T. F. Heinz, Ph.D. dissertation, University of California at Berkeley, 1982.

[23]R. G. Greenler, J. Chem. Phys. **44**, 310 (1966).

[24]H. Ibach, Surf. Sci. **66**, 56 (1977).

[25]B. N. J. Persson, Solid State Commun. **30**, 163 (1979).

[26]P. Hollins and J. Pritchard, Surf. Sci. **89**, 486 (1979).

[27]B. E. Hayden, K. Kretzschuman, and A. M. Bradshaw, Surf. Sci. **155**, 553 (1985).

[28]D. A. Kleinman, A. Ashkin, and G. D. Boyd, Phys. Rev. **145**, 338 (1966).

[29]J. Reutt-Robey, D. J. Doren, Y. J. Chabal, and S. B. Christman, Phys. Rev. Lett. **61**, 2778 (1988).